Ionic Crystals

DOI: 10.1002/ange.200702950

Gas-Conforming Transformability of an Ionic Single-Crystal Host Consisting of Discrete Charged Components

Satoshi Takamizawa, Takamasa Akatsuka, and Takahiro Ueda*

Tris(ethylenediamine)cobalt(III) chloride, $[Co^{III}(en)_3]Cl_3$ (en = ethylenediamine), is one of the most fundamental compounds of coordination chemistry. Although the well-known ethylenediamine complexes may be regarded as well studied, research that considers their gas-adsorbent ability has not been reported. The racemic hydrated crystal of (±)-$[Co(en)_3]Cl_3$ (**1**) includes H_2O molecules within the one-dimensional channels (see Figure 1).[1] Although the "zeolitic" behavior of **1** as a hydrate and dehydrate was reported in

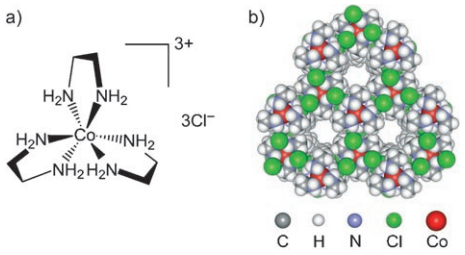

Figure 1. a) Structure of **1**; b) channel view of racemic crystal of **1**.

1959,[2] the gas-adsorption ability of dried crystals of **1** was recently euphemistically indicated in 2002 and 2003 by a solid-state NMR spectroscopic study of *n*-alkanes under saturated vapor as well as of loaded Xe gas at high pressure.[3] Currently, porous materials based on metal complexes are very attractive research targets owing to their designable structure, unusual flexibilities, and projected tunable functions.[4]

Dynamic porosity has been given much attention for the function of dynamic guest inclusion,[4–6] which can control guest reactivity and stability.[7] In the context of host dimensionality and binding forces for the component skeletons, currently the most actively investigated materials generally consist of polymeric skeletons with the assistance of van der Waals interpolymer interactions. Such structures should be well restricted in their transformability regarding the direction and range of motion by how the 3D architecture is constructed. Thus, an ionic crystal consisting of charged spherical components can be considered to possess extremely unrestricted transformability, which is regulated mostly by the minimization of the ionic-crystal energy under the various gas-adsorbing states. In this case, the Coulombic potential is rather "loose" in terms of binding interaction, which is generated in isotropic radial directions over a long distance proportional to r^{-1} (r = intermolecular distance), whereas that of van der Waals interactions is proportional to r^{-6}. Thus, there is a possibility that the ionic crystal can transform its crystal structure to sensitively adapt to the various adsorbed-guest properties even by weak physisorption. Because crystal **1** seems to satisfy these requirements for the target-flexible ionic porosity, we focus on the gas adsorbency of ionic crystal **1**. The purely van der Waals molecular crystal host is known for the cyclotriphosphazene inclusion compound.[8]

Well-formed hydrated single crystals of **1** ($[Co^{III}(en)_3]Cl_3 \cdot 4H_2O$) were obtained as hexagonal rods by recrystallization from water. The structure has 1D channels running along the rod axis perpendicular to the hexagonal (001) plane, forming a channel crystal with 1D penetration pores (Figure 2). Single-crystal X-ray diffraction analysis demonstrated the 1D channel structure of **1** including a 1D water chain with the infinite connectivity of a trigonal-bipyramidal periodic unit (Figure 3a). After vacuum drying at 60 °C, single-crystal X-ray diffraction analysis can be performed to determine the vacant-host structure of **1** (Figure 3b), even though the appearance of the dried crystals indicates imperfections (Figure 2b).

The dried crystal contains no water molecules, and the cell volume is 11 % less than that of the hydrated crystal while

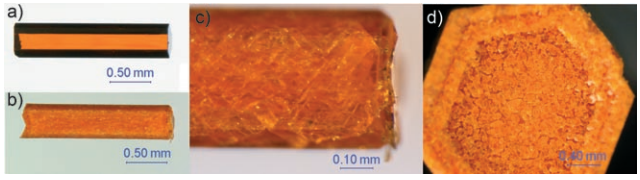

Figure 2. Photographs of typical hexagonal rod crystals of **1**: a) air-dried; b) vacuum-dried at 60 °C; c) magnified side view of the crystal in (b); d) magnified top view of the crystal. The dried crystals have many chaps with random cracks at the crystal sides (c), and tracing cracks were observed along the outlines of the hexagonal pieces at the top surface of the crystal (d). Thus, the dried crystal of **1** can be regarded as one kind of single-crystal state with imperfections that occurred while the single-crystal nature was maintained, as supported by mosaic-like cracks.

[*] Dr. S. Takamizawa, T. Akatsuka
International Graduate School of Arts and Sciences
Yokohama City University
Kanazawa-ku, Yokohama, Kanagawa 236-0027 (Japan)
Fax: (+81) 45-787-2187
E-mail: staka@yokohama-cu.ac.jp
Homepage: http://nanochem.sci.yokohama-cu.ac.jp
Dr. T. Ueda
Department of Chemistry, Graduate School of Science
Osaka University
Toyonaka, Osaka 560-0043 (Japan)
The Museum of Osaka University, Osaka University
Toyonaka, Osaka 560-0043 (Japan)

Supporting information for this article is available on the WWW under http://www.angewandte.org or from the author.

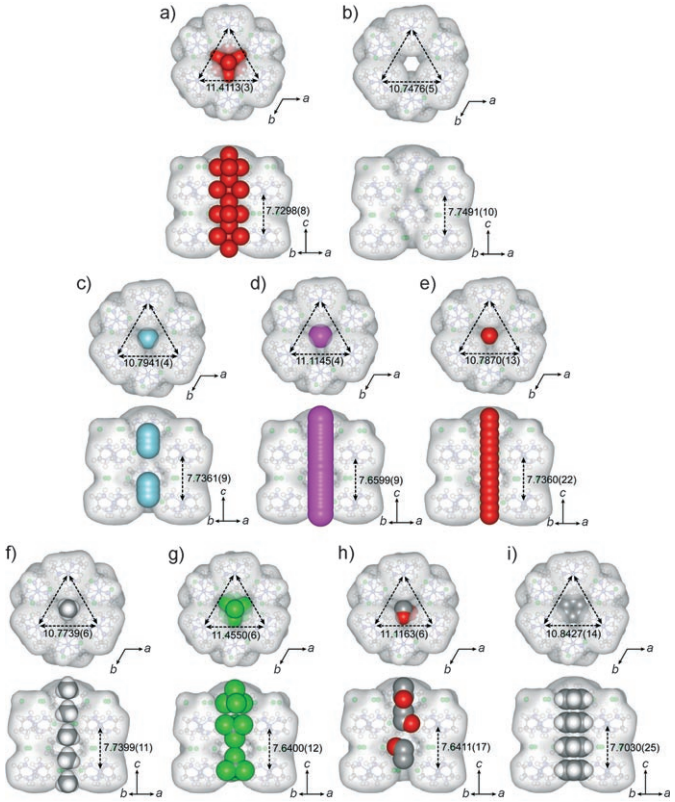

Figure 3. Channel view (surface model) of **1** with various guests (CPK model) accumulating through gas adsorption as determined by single-crystal X-ray diffraction analysis at 90 K. a) **1**·4 H_2O, b) dried **1**, c) **1**·0.13 Ar, d) **1**·0.64 Xe, e) **1**·0.55 O_2, f) **1**·0.75 CH_4, g) **1**·0.61 CCl_4, h) **1**·0.75 EtOH, i) **1**·C_6H_6; in each case, top view (upper structure) and side view (lower structure). Co–Co separations within the lattice are shown in Å.

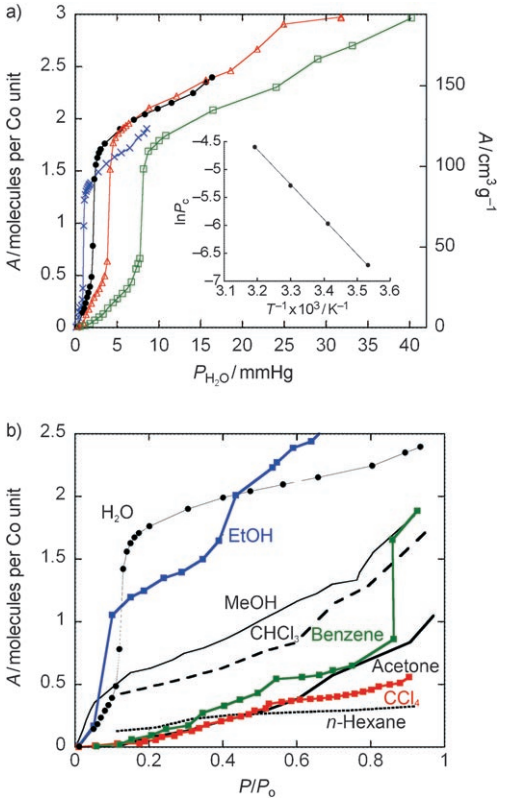

Figure 4. Vapor-adsorption isotherm curves of **1**: a) H_2O at 10 °C (blue cross), 20 °C (black solid circles), 30 °C (red triangles), and 40 °C (green squares); the right-hand axis shows the volume of adsorbed gas at standard temperature and pressure per gram of compound **1** (*A* indicates the adsorbed amount); inset: Clausius–Clapeyron plot using the starting pressure of the sharp adsorption increase at measurement temperatures. b) Adsorption of various vapors at 20 °C.

essentially the same structure is maintained. The resulting cell parameters indicate the narrowing of the channel diameter by removal of guest water molecules and diminishing along the *a* and *b* axes while the *c* parameter of the channel direction remains at almost the same value. Single-crystal X-ray diffraction analysis demonstrated that the dried crystal consistently recovers to the hydrated crystal by being exposed to water vapor although the imperfections in the crystals remained. These observations demonstrate the contraction and expansion of the diameter of the 1D channel of **1** during the de- and adsorption processes of water vapor in the channels of **1**.

Pressure-selective adsorption behavior was clearly observed in the water vapor adsorption isotherm measurements (Figure 4a). The adsorption curve has a sharp increase at around 0.1 relative pressure and then steadily reaches a saturated state. The critical relative pressure at which the sharp increases in adsorption occur shifts significantly higher as the temperature increases, which indicates that the adsorption enthalpy is larger than that of water condensation. An estimation by the Clausius–Clapeyron equation gives an adsorption enthalpy of 52.0 kJ mol^{-1} in **1** (inset in Figure 4a), which is slightly larger than that of bulk water condensation (44 kJ mol^{-1}), thus indicating the moderate hydrating and dehydrating ability of **1** not only by the Coulombic potential for the stabilization of adsorbed polar water molecules but also by reduction of the ionic character of $[Co(en)_3]^{3+}$ through the encapsulation of organic ligands. The abrupt increase in adsorption of water vapor by **1** indicates a "mass-induced phase transition,"[9] which suggests the reversible shrinkage and expansion of **1** through gas adsorption triggered by the formation of specific water aggregation as well as by the increased amount of adsorbed water.

Surprisingly, vapor-adsorbing ability of **1** was observed for various gases (Figure 4b). In measurements of organic-vapor adsorption at 20 °C, adsorption was clearly observed in a rather steady fashion, thus indicating the gradual transformation of the host to accommodate the organic vapor without an abrupt transition. Although adsorption of organic vapors was clearly observed at 293 K (20 °C), adsorption of small gases such as Ar, O_2, and N_2 was negligible at 77 K, and slight adsorption was observed for CO_2 at 195 K, which suggests the suppression of gas adsorption at low temperatures. This difficulty indicates the important role of thermally activated motion of the crystal host for gas diffusion in the adsorption process.[10]

The principal structures of the gas-inclusion states were determined by single-crystal X-ray diffraction analysis (Fig-

ure 3c–i). The adsorption of the light gases Ar, O_2, Xe, and CH_4 were successfully demonstrated in the structural analyses under pressured-gas conditions. However, the atomic gases of Ar and Xe and the dinuclear molecule of O_2 appear with multiple positions at the center of the channels, which indicate multiple stable sites in the channel for small gases. Interestingly, for the more complicated polyatomic guest molecules CH_4, EtOH, and benzene, the uncertainty in locating the guests within the channel decreased as the number of host–guest contact points increased. The adsorbed guests included in the 1D channels mainly interact with the methylene moieties of the en ligand on the channel surface, which suggests the important role of interatomic multipoint support between the host and guest for stabilizing guests inside the channel (see the Supporting Information).

As the guest size becomes larger, the channel begins expanding. The expansion in cell volume resulting from channel expansion seems to depend more on the accumulated guest volume than on the guest size itself, which is in good agreement with the gradual transformation suggested in the adsorption measurements. In the process of crystal expansion, a characteristic flexibility in the ionic-crystal host was found. Although crystal **1** exhibits rigid porosity when including the small gases of Ar, O_2, and CH_4, expansion was observed with larger included guests. Interestingly, in the comparison between spherical guests from CH_4, Xe, and CCl_4 (the size order is $CH_4 < Xe < CCl_4$, and the crystal composition is similar with **1**·0.74 CH_4, **1**·0.64 Xe, and **1**·0.61 CCl_4), lengths of their cell axes change anisotropically: *a*, which is related to channel diameter, increases from 10.7739(6) to 11.1145(4) to 11.4550(6) Å, respectively, and *c*, which is related to channel length, decreases from 15.4797(18) to 15.3199(11) to 15.2801(17) Å. These observations clearly relate channel shortening as well as channel expansion to guest expansion. This result shows that the crystal transformation of flexible ionic crystal **1** is mainly regulated by minimizing the ionic-crystal lattice energy resulting from the Coulombic binding force of the discrete components as well as van der Waals interactions. This free regulation seems to achieve the gradual host transformation and the cancellation of local structural distortion by distributing the adsorbed molecules within the comparatively extensive portion of the crystal **1**, thereby maintaining the single-crystal nature (cocrystallization) in adjusting a halfway state of incorporating various guests.

Since the host properties of ionic molecular crystals have not been explored in detail, the observed dynamic gas adsorption is meaningful. Systematic study of the transformable ionic-crystal host can be promoted by the stretch of **1** as a leading crystal since there is sufficient room for replacing and combining ionic components with various shapes, charges, and charge distributions.

Experimental Section

Compound **1** was synthesized according to a reported procedure,[1b] and well-shaped single crystals that were formed after recrystallization from hot water were used for all measurements. A crystal of **1** can easily grow as a large hexagonal rod on a centimeter scale. Gas-adsorption isotherm measurements were performed by a volumetric method (Autosorb 1, Quantachrome) after vacuum drying at 60 °C.

All single-crystal X-ray analyses were performed on a Bruker Smart APEX CCD area diffractometer with a nitrogen-flow temperature controller (Japan Thermal Eng. TC-10KCP) using graphite-monochromated $Mo_{K\alpha}$ radiation ($\lambda = 0.71073$ Å). All procedures for dried crystals were performed under moisture-free conditions. A dried single crystal of **1** was sealed in a glass capillary with pressurized gas or saturated vapor. In the case of argon (4.4 MPa), xenon (4.1 MPa), oxygen (5.8 MPa), and methane (4.8 MPa) gases, the inner pressure at room temperature was estimated by the ratio of the volumes of the condensed gases at 77 K and the pressure inside the capillary. Empirical absorption corrections were applied using the SADABS program. The structures were solved by direct methods (SHELXS-97) and refined by full-matrix least-squares calculations on $|F|^2$ (SHELXL-97) using the SHELXTL program package. Non-hydrogen atoms were refined anisotropically; hydrogen atoms were fixed at calculated positions and refined using a riding model. CCDC-645728 (**1**·4 H_2O as synthesized), 645729 (**1** after vacuum drying at 60 °C), 645730 (**1**·4 H_2O recovered by exposure to water vapor), 645731 (**1**·0.13 Ar), 645732 (**1**·0.64 Xe), 645733 (**1**·0.55 O_2), 645734 (**1**·0.74 CH_4), 645735 (**1**·0.61 CCl_4), 645736 (**1**·0.75 C_2H_5OH), and 645737 (**1**·C_6H_6) contain the supplementary crystallographic data for this paper. These data can be obtained free of charge from The Cambridge Crystallographic Data Centre via www.ccdc.cam.ac.uk/data_request/cif.

Received: July 3, 2007
Published online: November 6, 2007

Keywords: adsorption · host–guest systems · ionic crystals · solid-state structures · X-ray diffraction

[1] a) Y. Saito, K. Nakatsu, M. Shiro, H. Kuroya, *Acta Crystallogr.* **1955**, *8*, 729–730; b) K. Nakatsu, Y. Saito, H. Kuroya, *Bull. Chem. Soc. Jpn.* **1956**, *29*, 428–434; c) A. Whuler, C. Brouty, P. Spinat, P. Herpin, *Acta Crystallogr. Sect. B* **1975**, *31*, 2069–2075.

[2] a) H. Chihara, K. Nakatsu, *Bull. Chem. Soc. Jpn.* **1959**, *32*, 903–908; b) H. Chihara, *Bull. Chem. Soc. Jpn.* **1959**, *32*, 908–912.

[3] a) T. Ueda, T. Eguchi, N. Nakamura, R. E. Wasylishen, *J. Phys. Chem. B* **2003**, *107*, 180–185; b) T. Ueda, G. M. Bernard, R. McDonald, R. E. Wasylishen, *Solid State Nucl. Magn. Reson.* **2003**, *24*, 163–183; c) N. Nagaoka, T. Ueda, N. Nakamura, *Z. Naturforsch. A*, **2002**, *57*, 435-440.

[4] a) O. M. Yaghi, M. O'Keeffe, N. W. Ockwig, H. K. Chae, M. Eddaoudi, J. Kim, *Nature* **2003**, *423*, 705–713; b) S. Kitagawa, R. Kitaura, S. Noro, *Angew. Chem.* **2004**, *116*, 2388–2430; *Angew. Chem. Int. Ed.* **2004**, *43*, 2334–2375; c) G. Férey, C. Mellot-Draznieks, C. Serre, F. Millange, *Acc. Chem. Res.* **2005**, *38*, 217–225; d) D. Bradshaw, J. B. Claridge, E. J. Cussen, T. J. Prior, M. J. Rosseinsky, *Acc. Chem. Res.* **2005**, *38*, 273–282; e) W. Mori, S. Takamizawa in *Organometallic Conjugation* (Eds.: A. Nakamura, N. Ueyama, K. Yamaguchi), Kodansha Springer, Tokyo, **2002**, chap. 6, pp. 179–213.

[5] For example: a) C. Serre, F. Millange, C. Thouvenot, M. Nogues, G. Marsolier, D. Louër, G. Férey, *J. Am. Chem. Soc.* **2002**, *124*, 13519–13526; b) R. Kitaura, K. Seki, G. Akiyama, S. Kitagawa, *Angew. Chem.* **2003**, *115*, 444–447; *Angew. Chem. Int. Ed.* **2003**, *42*, 428–431; c) T. Loiseau, C. Serre, C. Huguenard, G. Fink, F. Taulelle, M. Henry, T. Bataille, G. Férey, *Chem. Eur. J.* **2004**, *10*, 1373–1382; d) K. Yamada, S. Yagishita, H. Tanaka, K. Tohyama, K. Adachi, S. Kaizaki, H. Kumagai, K. Inoue, R. Kitaura, H-C. Chang, S. Kitagawa, S. Kawata, *Chem. Eur. J.* **2004**, *10*, 2647–2660.

[6] a) S. Takamizawa, E. Nakata, T. Saito, K. Kojima, *CrystEngComm* **2003**, *5*, 411–413; b) S. Takamizawa, E. Nakata, H.

Yokoyama, K. Mochizuki, W. Mori, *Angew. Chem.* **2003**, *115*, 4467 – 4470; *Angew. Chem. Int. Ed.* **2003**, *42*, 4331 – 4334; c) S. Takamizawa, E. Nakata, T. Saito, *Inorg. Chem. Commun.* **2003**, *6*, 1415 – 1418; d) S. Takamizawa, E. Nakata, T. Saito, *Angew. Chem.* **2004**, *116*, 1392 – 1395; *Angew. Chem. Int. Ed.* **2004**, *43*, 1368 – 1371; e) S. Takamizawa, E. Nakata, T. Saito, *Inorg. Chem. Commun.* **2004**, *7*, 1 – 3; f) S. Takamizawa, E. Nakata, T. Saito, *Chem. Lett.* **2004**, *33*, 538 – 539; g) S. Takamizawa, E. Nakata, *CrystEngComm* **2005**, *7*, 476 – 479; h) S. Takamizawa, E. Nakata, T. Saito, T. Akatsuka, *Inorg. Chem.* **2005**, *44*, 1362 – 1366; i) S. Takamizawa, E. Nakata, T. Akatsuka, *Angew. Chem.* **2006**, *118*, 2274 – 2279; *Angew. Chem. Int. Ed.* **2006**, *45*, 2216 – 2221.

[7] a) M. Kawano, Y. Kobayashi, T. Ozeki, M. Fujita, *J. Am. Chem. Soc.* **2006**, *128*, 6558 – 6559; b) M. Yoshizawa, M. Tamura, M. Fujita, *Science* **2006**, *312*, 251 – 254; c) C. Kachi-Terajima, T. Akatsuka, M. Kohbara, S. Takamizawa, *Chem. Asian J.* **2007**, *2*, 40 – 50; d) S. Takamizawa, C. Kachi-Terajima, T. Akatsuka, M. Kohbara, T. Jin, *Chem. Asian J.* **2007**, *2*, 837 – 848.

[8] a) P. Sozzani, S. Bracco, A. Comotti, L. Ferretti, R. Simonutti, *Angew. Chem.* **2005**, *117*, 1850 – 1854; *Angew. Chem. Int. Ed.* **2005**, *44*, 1816 – 1820; b) P. Sozzani, A. Comotti, S. Bracco, R. Simonutti, *Angew. Chem.* **2004**, *116*, 2852 – 2857; *Angew. Chem. Int. Ed.* **2004**, *43*, 2792 – 2797; c) P. Sozzani, A. Comotti, R. Simonutti, T. Meersmann, J. W. Logan, A. Pines, *Angew. Chem.* **2000**, *112*, 2807 – 2810; *Angew. Chem. Int. Ed.* **2000**, *39*, 2695 – 2699.

[9] S. Takamizawa, T. Saito, T. Akatsuka, E. Nakata, *Inorg. Chem.* **2005**, *44*, 1421 – 1424.

[10] The necessity of the host crystal motion for gas adsorption has been indicated: a) S. Takamizawa, E. Nakata, T. Saito, *CrystEngComm* **2004**, *6*, 39 – 41; b) S. Takamizawa, M. Kohbara, *Dalton Trans.* **2007**, 3640 – 3645.

[11] Crystal data for **1**·4 H_2O as synthesized: 417.64 g mol^{-1}, trigonal, space group $P\bar{3}c1$, $T = 90$ K, $a = 11.4113(3)$, $c = 15.4595(8)$ Å, $V = 1743.40(11)$ Å^3, $Z = 4$, $\rho_{calcd} = 1.591$ Mg m^{-3}, $R_1 = 0.0387$ (0.0406), $wR_2 = 0.1027$ (0.1039) for 1370 reflections with $I > 2\sigma(I)$ (for 1453 reflections (11952 total measured)), goodness-of-fit on $|F|^2$ 1.084, largest diff. peak/hole 1.459/−1.419 e Å^{-3}; accessible volume of 385.7 Å^3 (22.1 %).

[12] Crystal data for **1** after vacuum drying at 60 °C: 345.59 g mol^{-1}, trigonal, space group $P\bar{3}c1$, $T = 90$ K, $a = 10.7476(5)$, $c = 15.4981(15)$ Å, $V = 1550.36(18)$ Å^3, $Z = 4$, $\rho_{calcd} = 1.481$ Mg m^{-3}, $R_1 = 0.0381$ (0.0530), $wR_2 = 0.0975$ (0.1110) for 1065 reflections with $I > 2\sigma(I)$ (for 1294 reflections (10091 total measured)), goodness-of-fit on $|F|^2$ 1.185, largest diff. peak/hole 1.043/−0.537 e Å^{-3}; accessible volume of 213.3 Å^3 (13.8 %).

[13] Crystal data for **1**·4 H_2O recovered by exposure to water vapor: 417.64 g mol^{-1}, trigonal, space group $P\bar{3}c1$, $T = 90$ K, $a = 11.4199(3)$, $c = 15.4590(8)$ Å, $V = 1745.97(11)$ Å^3, $Z = 4$, $\rho_{calcd} = 1.589$ Mg m^{-3}, $R_1 = 0.0427$ (0.0443), $wR_2 = 0.1149(0.1164)$ for 1392 reflections with $I > 2\sigma(I)$ (for 1457 reflections (11891 total measured)), goodness-of-fit on $|F|^2$ 1.068, largest diff. peak/hole 1.760/−1.225 e Å^{-3}; accessible volume of 386.4 Å^3 (22.1 %).

[14] Crystal data for **1**·0.13 Ar: 350.79 g mol^{-1}, trigonal, space group $P\bar{3}c1$, $T = 90$ K, $a = 10.7941(4)$, $c = 15.4722(12)$ Å, $V = 1561.19(15)$ Å^3, $Z = 4$, $\rho_{calcd} = 1.492$ Mg m^{-3}, $R_1 = 0.0338$ (0.0456), $wR_2 = 0.0902$ (0.0975) for 1086 reflections with $I > 2\sigma(I)$ (for 1300 reflections (10423 total measured)), goodness-of-fit on $|F|^2$ 1.202, largest diff. peak/hole 0.803/−0.258 e Å^{-3}; accessible volume of 222.1 Å^3 (14.2 %).

[15] Crystal data for **1**·0.64 Xe: 430.28 g mol^{-1}, trigonal, space group $P\bar{3}c1$, $T = 90$ K, $a = 11.1145(4)$, $c = 15.3199(11)$ Å, $V = 1638.95(14)$ Å^3, $Z = 4$, $\rho_{calcd} = 1.744$ Mg m^{-3}, $R_1 = 0.0304$ (0.0404), $wR_2 = 0.0802$ (0.0851) for 1134 reflections with $I > 2\sigma(I)$ (for 1365 reflections (11039 total measured)), goodness-of-fit on $|F|^2$ 1.157, largest diff. peak/hole 0.558/−0.565 e Å^{-3}; accessible volume of 304.4 Å^3 (18.6 %).

[16] Crystal data for **1**·0.55 O_2: 363.23 g mol^{-1}, trigonal, space group $P\bar{3}c1$, $T = 90$ K, $a = 10.7870(13)$, $c = 15.472(4)$ Å, $V = 1559.1(5)$ Å^3, $Z = 4$, $\rho_{calcd} = 1.547$ Mg m^{-3}, $R_1 = 0.0422$ (0.0576), $wR_2 = 0.1132(0.1282)$ for 1060 reflections with $I > 2\sigma(I)$ (for 1303 reflections (10279 total measured)), goodness-of-fit on $|F|^2$ 1.169, largest diff. peak/hole 1.018/−0.741 e Å^{-3}; accessible volume of 214.2 Å^3 (13.7 %).

[17] Crystal data for **1**·0.74 CH_4: 357.42 g mol^{-1}, trigonal, space group $P\bar{3}c1$, $T = 90$ K, $a = 10.7739(6)$, $c = 15.4797(18)$ Å, $V = 1556.1(2)$ Å^3, $Z = 4$, $\rho_{calcd} = 1.526$ Mg m^{-3}, $R_1 = 0.0384$ (0.0505), $wR_2 = 0.1074$ (0.1165) for 1083 reflections with $I > 2\sigma(I)$ (for 1298 reflections (10234 total measured)), goodness-of-fit on $|F|^2$ 1.268, largest diff. peak/hole 1.190/−0.543 e Å^{-3}; accessible volume of 213.3 Å^3(13.7 %).

[18] Crystal data for **1**·0.61 CCl_4: 439.50 g mol^{-1}, trigonal, space group $P\bar{3}c1$, $T = 90$ K, $a = 11.4550(6)$, $c = 15.2801(17)$ Å, $V = 1736.4(2)$ Å^3, $Z = 4$, $\rho_{calcd} = 1.681$ Mg m^{-3}, $R_1 = 0.0352$ (0.0620), $wR_2 = 0.0832(0.1035)$ for 1102 reflections with $I > 2\sigma(I)$ (for 1459 reflections (11321 total measured)), goodness-of-fit on $|F|^2$ 1.177, largest diff. peak/hole 0.772/−0.701 e Å^{-3}; accessible volume of 376.7 Å^3 (21.7 %).

[19] Crystal data for **1**·0.75 C_2H_5OH: 380.13 g mol^{-1}, trigonal, space group $P\bar{3}c1$, $T = 90$ K, $a = 11.1163(6)$, $c = 15.2822(16)$ Å, $V = 1635.4(2)$ Å^3, $Z = 4$, $\rho_{calcd} = 1.544$ Mg m^{-3}, $R_1 = 0.0556$ (0.0786), $wR_2 = 0.1428$ (0.1673) for 747 reflections with $I > 2\sigma(I)$ (for 971 reflections (8274 total measured)), goodness-of-fit on $|F|^2$ 1.199, largest diff. peak/hole 0.786/−0.312 e Å^{-3}; accessible volume of 305.5 Å^3 (18.7 %).

[20] Crystal data for **1**·C_6H_6: 423.70 g mol^{-1}, trigonal, space group $P\bar{3}c1$, $T = 90$ K, $a = 10.8427(14)$, $c = 15.406(4)$ Å, $V = 1568.6(5)$ Å^3, $Z = 4$, $\rho_{calcd} = 1.794$ Mg m^{-3}, $R_1 = 0.0529$ (0.0733), $wR_2 = 0.1532$ (0.1745) for 747 reflections with $I > 2\sigma(I)$ (for 929 reflections (7600 total measured)), goodness-of-fit on $|F|^2$ 1.266, largest diff. peak/hole 2.443/−0.566 e Å^{-3}; accessible volume of 235.4 Å^3 (15.0 %).

